Palaeoentomology 007 (5): 628–637
https://www.mapress.com/pe/

Article

ISSN 2624-2826 (print edition)
PALAEOENTOMOLOGY
ISSN 2624-2834 (online edition)

https://doi.org/10.11646/palaeoentomology.7.5.6
http://zoobank.org/urn:lsid:zoobank.org:pub:DCEF8BB6-B121-4F20-A507-4DEC83524D3C

Arthropod coprolites and wound reaction in the late Paleozoic climbing fern *Hansopteris*

FENG-YAN LI[1, 2], ZHUO FENG[3], JOSEF PŠENIČKA[1, 4], JUN WANG[1, 2] & WEI-MING ZHOU[1,2]*

[1]*State Key Laboratory of Palaeobiology and Petroleum Stratigraphy, Nanjing Institute of Geology and Palaeontology, Chinese Academy of Sciences, No. 39 East Beijing Road, Nanjing 210008, China*
[2]*University of Chinese Academy of Sciences, No. 19(A) Yuquan Road, Beijing 100049, China*
[3]*Institute of Palaeontology, Yunnan Key Laboratory of Earth System Science, Yunnan Key Laboratory for Palaeobiology, MEC International Joint Laboratory for Palaeobiology and Palaeoenvironment, Yunnan University, Kunming 650500, China*
[4]*Centre of Palaeobiodiversity, West Bohemian Museum in Pilsen, Kopeckého sady 2, Plzeň 30100, Czech Republic*

3180100530@zju.edu.cn; https://orcid.org/0000-0003-1530-1861
zhuofeng@ynu.edu.cn; https://orcid.org/0000-0001-9635-1144
jpsenicka@zcm.cz; https://orcid.org/0000-0001-9240-9206
jun.wang@nigpas.ac.cn; https://orcid.org/0000-0002-2193-2195
wmzhou@nigpas.ac.cn; https://orcid.org/0000-0001-6190-6234
**Corresponding author*

Abstract

Interactions between arthropods and plants have been documented extensively in late Paleozoic trees and ground cover plants, but they have rarely been recorded in late Paleozoic climbers. In this study, we present the second example of coprolites preserved within the plant tissue from the early Permian fossil Lagerstätte Wuda Tuff Flora. The host axis is identified as a phyllophore of the climbing fern *Hansopteris uncinatus* by the combined evidence of anatomy, morphology, and associated plants. Unlike the first coprolites, which were suggested to be produced by oribatid mites, the culprit of the studied coprolites was likely a myriapod or beetle, indicated by their slightly larger size and the boring behaviour. Furthermore, anomalous parenchymatous cells, sclerenchymatous cells, and metaxylem tracheids have been observed surrounding the tunnel, suggesting responses to traumatic stimulus caused by arthropod damage. This discovery provides an informative example of arthropod herbivory on late Paleozoic climbers and sheds light on how the host plant responded during the early stage of injury.

Keywords: plant-arthropod interaction, boring tunnel, traumatic stimulus, fossil climber, pyrite framboid, Wuda Tuff Flora

Introduction

Interactions between plants and arthropods, the two major groups of macroorganisms with respect to Earth's biodiversity, constitute the dominant consumer pathway in terrestrial ecosystems, both in the modern world and throughout geological history. These interactions can be traced back to the late Silurian and Early Devonian periods, coinciding with the establishment of vascular plants on land (Scott *et al*., 1992). Throughout the late Paleozoic era, these interactions underwent rapid evolution, leaving numerous traces in the fossil record. These include evidence of feeding traces, such as consuming damage in leaves and wood-borings (Scott *et al*., 1992; Fletcher & Salisbury, 2014; Feng *et al*., 2017, 2019), and digestive residues of arthropods, such as coprolites and gut contents (Slater *et al*., 2012; Dunlop & Garwood, 2017). The consumption of plants by arthropods can be broadly categorized into two types: detritivory, in which arthropods attack the dead tissues of plants, and herbivory, in which arthropods attack the living tissues of plants. Herbivory, emerging later than detritivory in terrestrial ecosystems, involves more complex interactions and a higher probability of co-evolution between plants and arthropods (Labandeira, 2006).

It is widely accepted that extant ferns exhibit much higher resistance to herbivorous arthropods compared to seed plants (Hendrix, 1980; Fang *et al*., 2021). However, ferns during the late Paleozoic did not seem to enjoy such fortune. Coprolites of arthropods have been documented within various organs of Paleozoic ferns, including the stem (Rex, 1986; Labandeira *et al*., 1997), rachis (D'Rozario *et al*., 2011; Cheng *et al*., 2021; Feng *et al*., 2021), mesophyll (Zhou *et al*., 2022b), and sporangia

 Submitted: 25 Jun. 2024; accepted by D.-Y. Huang: 13 Oct. 2024; published: 30 Oct. 2024

(Slater *et al*., 2012), indicating a broad spectrum of interactions between ferns and arthropods. The occurrence of stem-borings surrounded by wound tissue in Paleozoic ferns, such as *Psaronius* (Lesnikowska, 1990; Scott *et al*., 1992), records the activity of herbivorous borers. Stylet probes found within *Psaronius* rachises demonstrate that tree ferns were victims of piercing-and-sucking arthropods during the late Paleozoic (Labandeira & Phillips, 1996). Recently, axis-borings in a fern (*Nemejcopteris haiwangii*) have been documented in the early Permian Wuda Tuff Flora (Feng *et al*., 2021; Pšenička *et al*., 2021).

Plant growth habits have been rarely considered in previous studies of plant-arthropod interactions. However, during the late Paleozoic, ferns encompassed a remarkable diversity in growth habits. This diversity allowed them to occupy various ecological niches, with climbing ferns playing distinct roles compared to tree ferns or ground cover ferns. In this paper, we present evidence of herbivory occurring in a climbing fern phyllophore from the early Permian Wuda Tuff Flora. This evidence—including a bored tunnel filled by coprolites and the wound reaction of plant tissue to the arthropod attack—contributes to a more comprehensive understanding of the interactions between ancient plants and arthropods.

Material and methods

The specimens were collected from a tuff bed within the uppermost Taiyuan Formation in the Wuda Coalfield of Inner Mongolia, China. The tuff bed is positioned between the No. 6 and No. 7 coal seams and preserves a peat-forming forest known as the "Wuda Tuff Flora" or the Chinese "vegetational Pompeii". The absolute age of the tuff bed was determined to be 298.34 ± 0.09 Ma through high-precision U-Pb dating of zircons (Schmitz *et al*., 2021). Numerous upright stumps in the outcrop indicate this forest community was buried *in situ*. Accordingly, plant fossils were meticulously collected and documented in various excavations, following a methodology based on 1 m^2 quadrats (Wang *et al*., 2021). The high-fidelity preservation of the forest structure has provided compelling evidence for interpreting the growth habits and plant-plant interactions of ferns (Zhou *et al*., 2019; Zhou *et al*., 2022a).

For examination of gross morphology, the specimen underwent immersion in 95% alcohol and was then photographed using a digital NIKON D-800 camera. In areas where three-dimensional anatomy was preserved, transverse and longitudinal sections were prepared meticulously using the EXAKT-300CP cutting system, followed by an EXAKT-400CS grinder. These sections were then photographed using either the stereomicroscope Zeiss Axio Zoom V16 or the microscope Zeiss Axio Imager Z2. The latter was equipped with an X-Cite 120Q fluorescence microscope excitation system for additional fluorescence imaging. Abnormal spheroidal structures were observed using scanning electron microscopes, either TESCAN MAIA 3 GMU or SU 3500, with the former also employed for scanning electron microscopy-energy-dispersive X-ray spectroscopy (SEM-EDS) analysis.

Results

On the specimen surface, the central area features a fragmentary main axis, measuring over 64 mm long and approximately 3 mm wide (Fig. 1A). Adjacent to the main axis is a slightly narrower extension, estimated at 2 mm wide, which appears to extend from the main axis and may be distorted at its proximal end. However, no other subordinate pinnae or branches have been found attached along the preserved length of the main axis. The surface of the main axis displays numerous circular scars, likely remnants of hairs or trichomes.

The middle part of the main axis, measuring 31 mm long, preserves three-dimensional anatomy (Fig. 1B). From this segment, six transverse sections (Fig. 1C–H) and a longitudinal section (Fig. 1I) have been prepared. Anatomically, the cortex of the main axis can be divided into two zones: a 0.2 mm-thickness outer zone consisting of sclerenchymatous cells 10–20 μm long and a >0.12 mm-thick inner zone consisting of parenchymatous cells 20–60 μm in diameter. In longitudinal section, the outer zone lacks distinct cell outlines, whereas the inner zone contains square to rectangular cells with noticeably thin walls.

The vascular configuration of the main axis displays some variations including: 1) a C-shaped xylem strand composed of a thin median region (perhaps due to the incompletely preserved tracheids) and two curved arms (Fig. 1D); 2) a C-shaped xylem strand composed of a thick median region and two curved arms (Fig. 1E); and 3) a C-shaped xylem strand composed of a thick median region and two recurved arms (Fig. 1C, F–H). In all three types, the median region consists of metaxylem tracheids (70–160 μm diameter) apparently larger than those of lateral arms (20–90 μm diameter). Additionally, a poorly-preserved protruding sclerenchymatous strand originates from the cortex and extends into the interior of the xylem concavity (Fig. 1C, E–H). There are four protoxylem groups present on the convex side of the xylem strand. The inner two groups are located on each connected portion between the median region and lateral arm, and the outer two groups are positioned in the middle of each lateral arm (Fig. 1C, D, F–H). No divergent pinna trace has been observed in these sections.

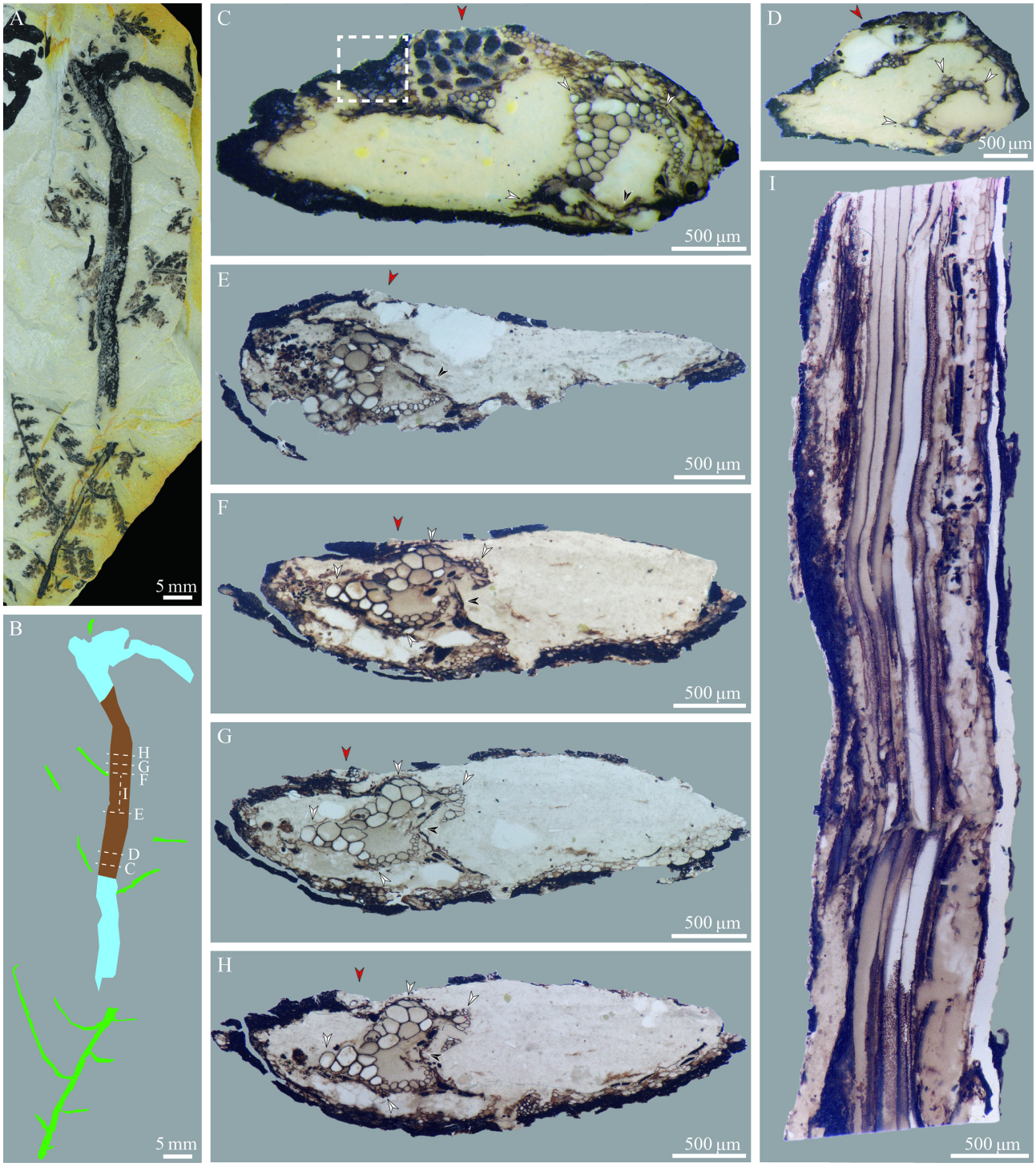

FIGURE 1. Gross morphology and anatomy of the main axis. **A**, The main axis and associated plant fragments, specimen PB204971. **B**, Diagram of **A**. Blue colour indicates the region preserved as impression; brown colour indicates the region with three-dimensional anatomy; green colour indicates the associated fronds. **C**–**H**, Six transverse sections of the main axis, showing the anatomical change of the xylem strand and the boring tunnel within the cortex. White arrows indicate the protoxylem groups; black arrows indicate the poorly-preserved protruding sclerenchymatous strand; red arrows indicate the boring hole. Dotted rectangular box in **C** highlights the area containing anomalous sclerenchymatous cells, which is magnified in Fig. 2C. **I**, Longitudinal section of the main axis.

A large cavity is found within the cortex (Figs 1C–H, 2A, B). In the transverse section illustrated in Fig. 2A, the cavity is oval and measures 680 × 500 µm. In another transverse section illustrated in Fig. 2B, the cavity is elongated and measures 1500 × 400 µm in size. The border of the cavity is generally smooth, with

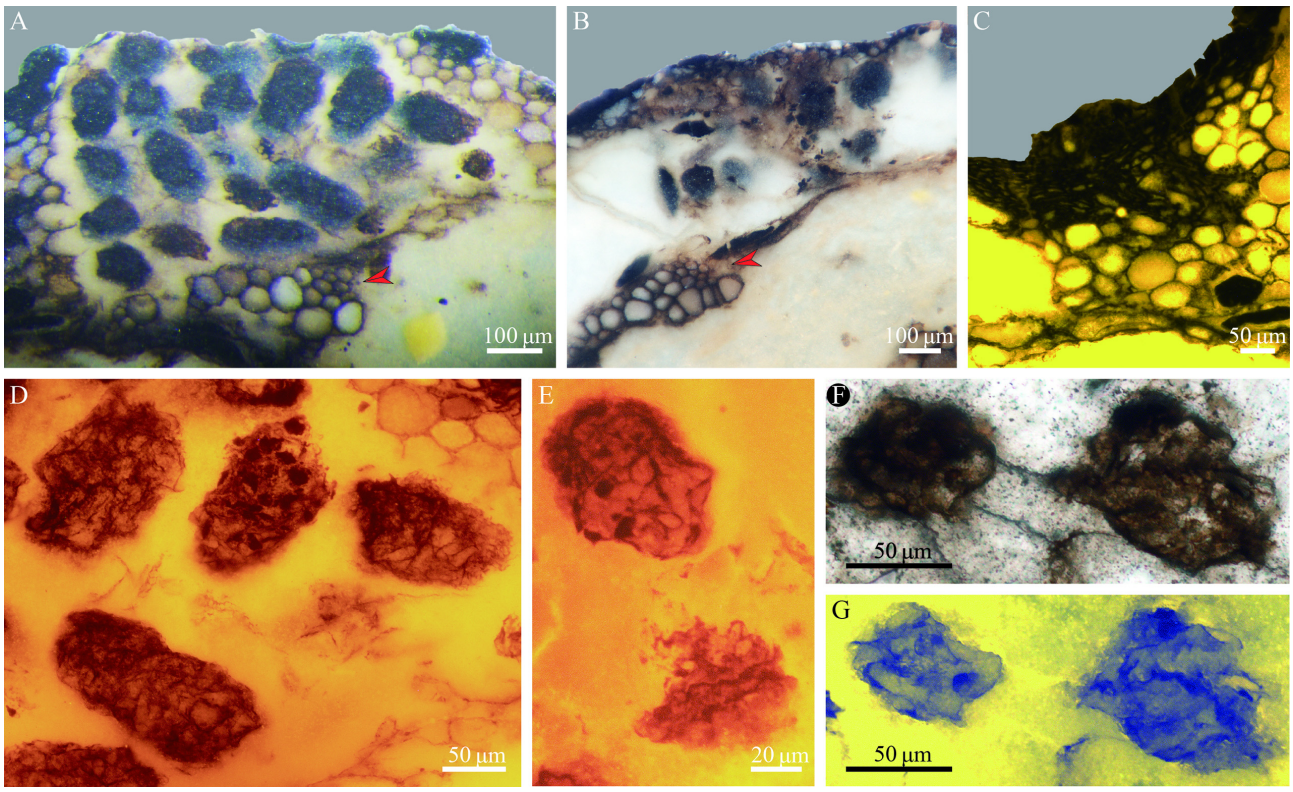

FIGURE 2. The boring tunnel and coprolites. **A**, Enlargement of Fig. 1C, showing the boring hole fully filled with coprolites, red arrow indicates the area with smaller parenchymatous cells. **B**, Enlargement of Fig. 1D, showing the boring hole filled with reduced number of coprolites, red arrow indicates the area with smaller parenchymatous cells. **C**, Enlargement of the rectangular box in Fig. 1C under fluorescence, showing anomalous sclerenchymatous cells invading into the inner layer of the cortex. **D**, Enlargement of **A** under fluorescence, showing coprolites consisting of undigested plant tissues. **E**, Enlargement of Fig. 1D under fluorescence, showing coprolites composed of undigested plant tissues. **F**, **G**, Enlargement of Fig. 1G, showing the fragmentary coprolites.

the peripheral parenchymatous cells exhibiting various fragmentary skeletons of cell walls (Fig. 2A, C). Several black bodies are preserved within the cavity (Fig. 2D, E). These bodies are in ovoidal to cylindrical forms, ranging from 110 × 60 μm to 180 × 80 μm. Under fluorescence, these bodies exhibit an uneven surface, and contain some inner structures. The morphology and size of these inner structures are similar to the surrounding parenchymatous cell walls, demonstrating them to be of undigested plant tissues. Therefore, the cavity is indicated to be a bored hole filled with coprolites. In a few cases, smaller bodies with irregular outlines are also found beyond the bored hole, in locations close to the vascular strand (Fig. 2F, G). They appear to be fragments crushed from more completely preserved coprolites.

Numerous circular structures, 10–30 μm in diameter, have been identified in both the parenchymatous cortex and the xylem strand, observed in both transverse and longitudinal sections (Fig. 3A–F). SEM-EDS analysis indicates that some of these circular structures were empty holes, later filled by the carbonaceous adhesive resin in the process of slice preparation (Fig. 3H–J); others are indicated to be the impressions of spheres (Fig. 3B, D, J). In a few cases, square crystals with side lengths of 2–4 μm are preserved within the spheroidal holes (Fig. 3D, J). The crystals mainly consist of the elements Fe and S (Fig. 3M, N).

Several tripinnate or bipinnate frond fragments were found in close proximity to the main axis (Figs 1A, 4A). These fronds, identifiable as belonging to a single species, are distinguished by their consistent pinnule morphology and the presence of circular reproductive organs. The antepenultimate rachis is approximately 1 mm in width with a smooth surface (Fig. 4A). The penultimate pinnae are over 25 mm long without a visible distal end (Fig. 4A). The ultimate pinnae typically consist of 7–9 pinnules arranged alternately (Fig. 4B). The pinnules have sphenopterid characteristics with sparse venation, each terminating in a single marginal tooth (Fig. 4B). Several circular reproductive organs, approximately 1 mm in diameter, are individually attached to or associated with the apex of pinnules (Fig. 4C). In addition, albeit

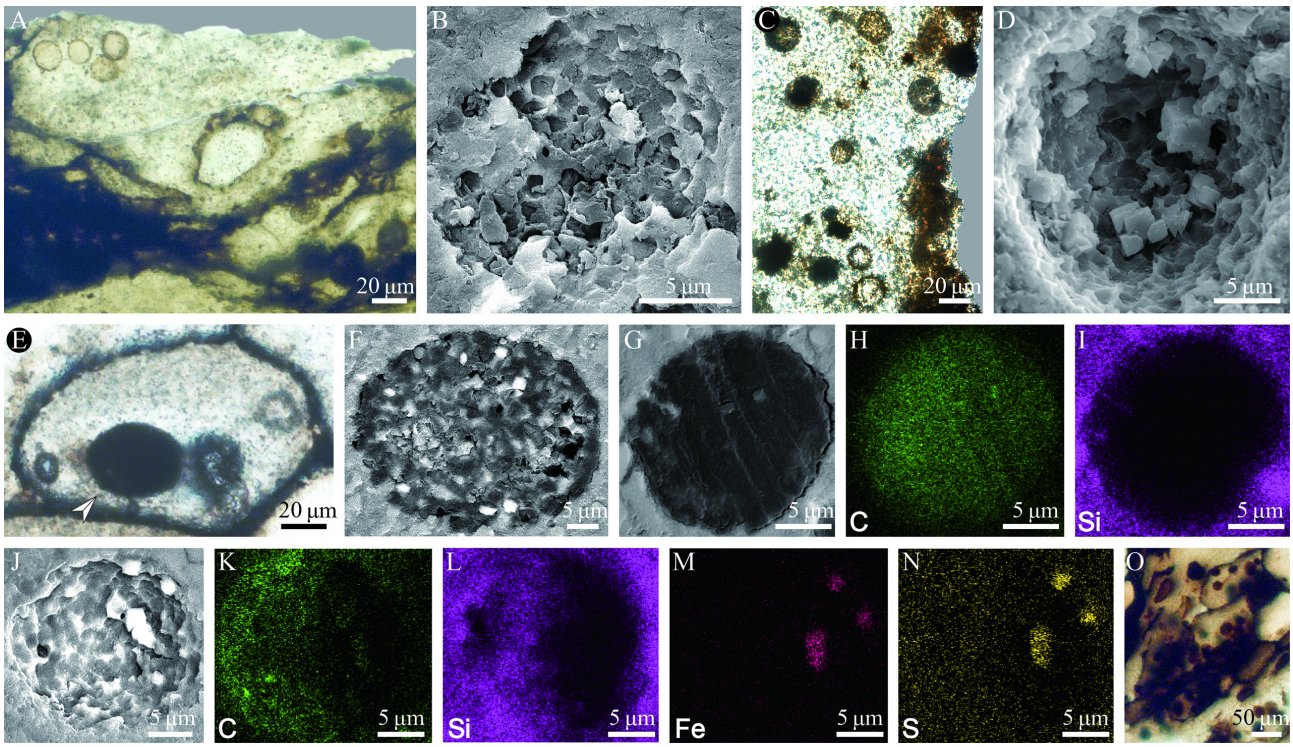

FIGURE 3. Small spherical structures within the main axis. **A**, Enlargement of Fig. 1G, showing their morphology in transverse section. **B**, A spherical structure from Fig. 1G observed under SEM, with numerous imprints of pyrite crystals. **C**, Enlargement of Fig. 1I, showing their morphology in longitudinal section. **D**, A spherical depression from Fig. 1I observed under SEM, showing several pyrite crystals preserved therein. **E**, Four spherical structures preserved within a tracheid. **F**, The largest spherical structure from **E** (white arrow) observed under SEM. **G**, A spherical structure from Fig. 1G observed under SEM, showing the empty hole later filled with the carbonaceous adhesive resin. **H**, **I**, Element maps of **G** for Carbon and Silicon respectively. **J**, A spherical structure from Fig. 1G observed under SEM, with remains of pyrite crystals. **K**–**N**, Element maps of **J** for Carbon, Silicon, Iron, and Sulfur respectively. **O**, Small circular structures re-examined in a previous section of *Hansopteris uncinatus* (Zhou *et al*., 2021).

incomplete, an aphlebia with three preserved lobes, seemingly formed by dichotomy (Fig. 4D), is located near the base of a penultimate pinna.

Discussion

Identification of the host plant

Anachoropterids are an inversicatenalean group of filicalean ferns distinguished by a C-shaped xylem strand with abaxially curved lateral arms and convexly positioned protoxylem groups (Galtier & Phillips, 2014). The studied main axis possesses this distinct anatomical feature, indicating its affinity with anachoropterids. To date, two anachoropterid species have been documented in the early Permian Wuda Tuff Flora. One, *Hansopteris uncinatus* Zhou, Pšenička, Bek, Wan, Boyce & Wang, features a U-shaped xylem strand in the antepenultimate rachis, with lateral arms composed of large metaxylem tracheids (Zhou *et al*., 2021). The other likely represents a new species of *Hansopteris* Zhou, Pšenička, Bek, Wan, Boyce & Wang, sharing significant similarities with *H. uncinatus* in gross morphology, but differing in possessing a bar-shaped xylem strand for the antepenultimate rachis (Zhou *et al*., 2022a). Although the studied main axis has some variations in xylem configuration, none is identical to that of the antepenultimate rachis of the two *Hansopteris* species.

The fragmentary fronds associated with the studied main axis are noteworthy due to their circular reproductive organs, which bear resemblance to those documented in *Hansopteris uncinatus* (Zhou *et al*., 2021). Notably, a new specimen collected from the same quadrat as the studied main axis (both specimens marked "24I") has similar fronds with circular reproductive organs (Fig. 4E). Fortunately, a frond on this specimen possesses three-dimensional anatomy in part of its antepenultimate rachis. The transverse section of the antepenultimate rachis reveals a U-shaped xylem strand with lateral arms comprising typical large-sized metaxylem tracheids (Fig. 4F), confirming the frond to be *H. uncinatus*.

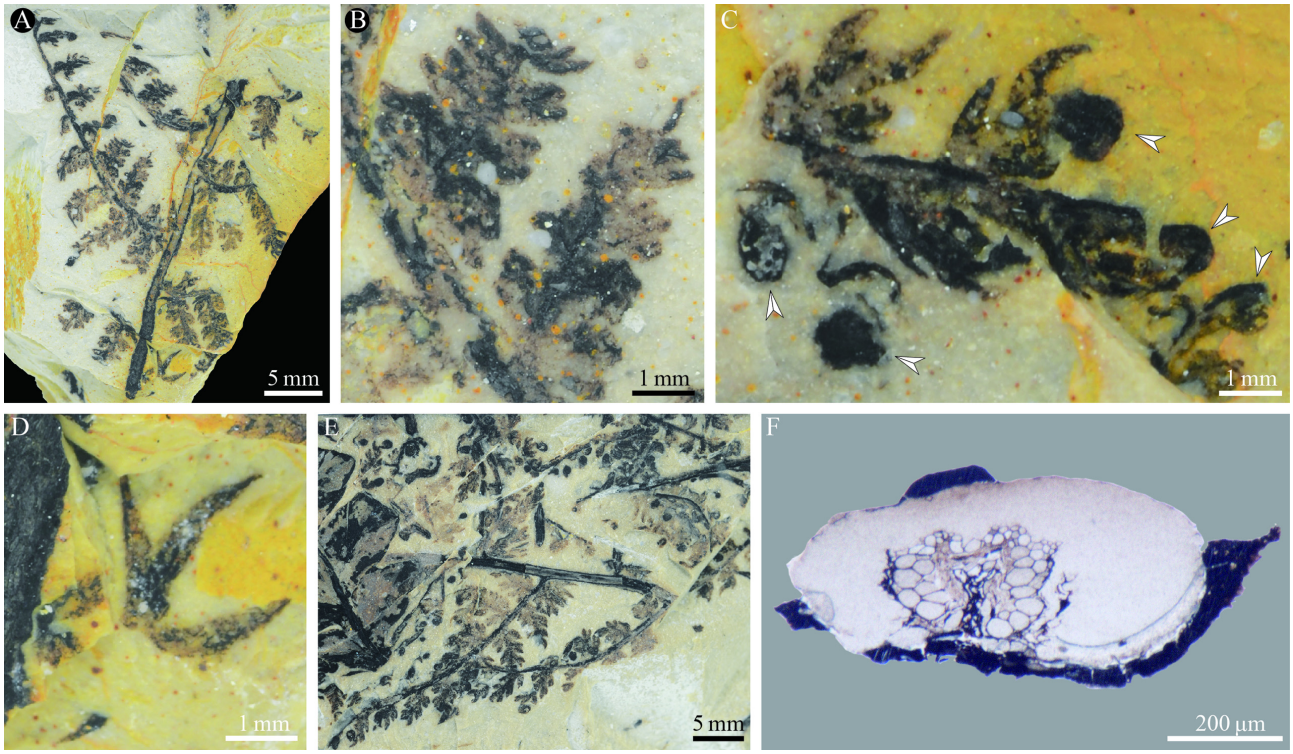

FIGURE 4. Associated fronds from the same quadrat. **A**, Enlargement of Fig. 1A, showing a tripinnate frond preserved on the same slab surface with the main axis. **B**, Enlargement of **A**, showing the morphology of two ultimate pinnae. **C**, Enlargement of Fig. 1A, showing a fragmentary pinna preserved on the same slab surface with the main axis, note the circular reproductive organs (white arrows). **D**, Enlargement of **A**, showing the aphlebia structure. **E**, Another specimen collected from the same quadrat, showing fronds identical to those of Fig. 1A, specimen PB204972. **F**, A transverse section made from the antepenultimate rachis arrowed in **E**, showing the rachis anatomy identifiable to *Hansopteris uncinatus*.

Considering the close proximity between the studied main axis and the fronds of *Hansopteris uncinatus*, particularly in the context of the *in-situ* preservation of the fossil forest which experienced limited transportation, we think it highly probable that the studied main axis also belongs to *H. uncinatus* rather than representing a new anachoropterid species. Additionally, the studied main axis exhibits a significantly larger width (3 mm) compared to the antepenultimate rachis (1 mm) in the associated fronds of *H. uncinatus*. The disparities in both size and anatomy suggest that the main axis likely represents a lower order structure from which the antepenultimate rachis originates. The studied main axis can be further interpreted as a "phyllophore" structure since only one lateral branch has been observed along the total 64 mm length (Fig. 1A) and no pinna trace has been found in the serial transverse sections (Fig. 1C–H).

Hansopteris uncinatus is a typical tendril-climbing fern in the Wuda Tuff Flora (Zhou *et al*., 2021). Few serving as hosts for arthropod coprolites have been documented through geological history, with only a few examples known among Pennsylvanian climbers, such as *Ankyropteris* (Sterzel) Bertrand and *Callistophyton* Delevoryas & Morgan (Rößler, 2000). The present discovery of coprolites preserved within the phyllophore of *H. uncinatus* expands our knowledge of this interaction, showing its persistence into the early Permian. In modern forests, climbing plants not only use their hosts for support but also face the risk of being scapegoated for arthropod attacks by the trees themselves, or conversely, trees may foster symbiotic arthropods to deter climbers (Putz, 1980). However, the origin and ecological impact of this interaction between tree hosts, climbing plants, and herbivorous arthropods in the fossil record remains uncertain.

Plant response to arthropod damage

Plants can respond to arthropod herbivory actively or passively as part of their defense mechanisms against biotic stress. Biotic stress, particularly caused by pathogens, such as bacteria, viruses, fungi, arthropods, and nematodes, triggers significant changes in plant hormones and related gene expression, leading to the formation of healing tissues (Nejat & Mantri, 2017). Throughout the late Paleozoic, wound reactions have been widely documented in various

plant organs, including stems, leaves, petioles, and roots. The damage and healing processes can occur within the cortex, vascular band, or even the pith. Several types of wound reactions have been observed, including but not limited to: 1) Vesicle-like outgrowths of parenchymatous cells (Holden, 1931; Feng *et al*., 2017); 2) Proliferation of parenchymatous cells (Holden, 1910, 1931; Lesnikowska, 1990; Feng *et al*., 2019); 3) Proliferation of tracheids (Stopes, 1907; Falcon-Lang *et al*., 2015); and 4) Protective layer formed by cells with thickened walls (Holden, 1912, 1931; Weaver *et al*., 1997).

In the studied main axis, arthropod damage occurs mainly within the cortex, represented by a bored tunnel with coprolites concentrated mainly at one end (Figs 1C–F, 2A, B). The parenchymatous cells surrounding the tunnel express some degree of proliferation, as indicated by the gradually diminished size of parenchymatous cells in the truncated portion (Fig. 2A, B). However, this pattern appears to be different from previously documented cases, where the tunnel was filled by regular rows of parenchymatous cells (Holden, 1910, 1931; Lesnikowska, 1990; Feng *et al*., 2019). Notably, sclerenchymatous cells typically constituting the outer layer of the cortex invade some distance into the inner layer of the cortex, replacing the larger-sized parenchymatous cells (Fig. 2C). This inward invasion likely aimed to form a sclerenchyma layer around the wound area, serving as a barrier against potential microbial infections. This barrier would help prevent the loss of water and nutrients, along with the spread of toxic substances (Holden, 1912; Kim *et al*., 2004; Ozeretskovskaya *et al*., 2009). It is plausible that the wound reaction in the main axis of the present fern occurred shortly before its burial in the tuff bed, given that the anomalous parenchymatous and sclerenchymatous cells appear to be in an initial stage of proliferation.

The characteristic of metaxylem tracheids in the median region being apparently larger in diameter and forming more layers than those in the lateral arms is indeed noteworthy, as this trait has never been reported in other specimens of *Hansopteris uncinatus* or any other known anachoropterid species (Galtier & Phillips, 2014; Zhou *et al*., 2021). A possible explanation is that this might represent a unique type of foliar anatomy, as different orders of anachoropterid axes may have had variation in xylem configuration (Zhou *et al*., 2024). However, a more plausible explanation is that the metaxylem tracheids towards the bored area became hyperplasic and hypertrophic due to traumatic stimulus. Similar wound reaction has been documented previously in a Pennsylvanian cordaitalean branch (Falcon-Lang *et al*., 2015).

Possible producer of the coprolites

The present study represents the second fossil record of coprolites preserved within plant tissues in the early Permian Wuda Tuff Flora, the first record being recently identified as coprolites remaining in the mesophyll of the fern *Botryopteris sinensis* Zhou, Pšenička, Bek, Libertín, Wang & Wang (Zhou *et al*., 2022b, 2023a, b). Previous taphonomic interpretations suggest that plant fragments preserved in a mass within the basal 30 mm of the tuff bed belong to the litter layer of the swamp forest community, whereas others preserved more widely separated from each other and in higher layers of the tuff bed were directly broken off from the main body and rapidly buried by volcanic ash (Zhou *et al*., 2022b). Therefore, these coprolites and some types of feeding traces were suggested to be formed by herbivory rather than detritivory (Feng *et al*., 2021; Zhou *et al*., 2022b). The present studied coprolites were also likely formed by herbivory, given their apparent preservation not in the litter layer. This argument is further supported by the fact that these coprolites were concentrated at one end and gradually diminished at the other end of the tunnel (Figs 1C–F, 2A, B), suggesting preservation in an upright orientation subjected gravity settling during the organism's lifetime. Moreover, the host plant exhibits reactions to the boring damage, providing convincing evidence for the interpretation of herbivory.

The size and texture of coprolites are often used to infer the producer (Scott & Taylor, 1983). In the mesophyll of *Botryopteris sinensis*, coprolites with smooth surface are typically circular to oval in cross-section, with a long axis mostly less than 110 μm, suggesting they were produced by oribatid mites (Zhou *et al*., 2022b). However, in the present studied specimen, most coprolites are ovoidal to cylindrical, with uneven surface and long axes ranging from 110 to 180 μm. These coprolites have sizes close to the upper limit of those of oribatid mites and springtails, and the lower limit of those of myriapods and holometabolous insects (Scott & Taylor, 1983; Labandeira *et al*., 1997). Oribatid mites and springtails primarily serve as decomposers in modern forest ecosystems, but they may also feed on living plant matter (Scott & Taylor, 1983). Nevertheless, they are unlikely to be the producer since oribatid mites normally produce coprolites with a smooth surface and a much smaller diameter (commonly <100 μm) (Scott & Taylor, 1983; Labandeira *et al*., 1997), and springtails lack the appropriate mouthpart structure to produce tunnels (Goto, 1972; Labandeira *et al*., 1997). In contrast, late Paleozoic myriapods and holometabolous insects, especially beetles (Feng *et al*., 2019; Cai *et al*., 2022), have been well-documented to be capable of producing boring tunnels through consumption of either decaying (D'Rozario *et al*., 2011; Rößler *et al*., 2012) or

living tissues (Feng *et al*., 2017, 2019; Wei *et al*., 2019; Laaß *et al*., 2020). The producer of the studied coprolites is likely to have been a small myriapod or beetle larva. However, the exact identity of the producer remains unknown due to the absence of body fossil evidence.

Initially, the spheroidal structures in both longitudinal and transverse sections (Fig. 3A, C, E) were assumed to be fungi, as fungal spores with similar morphology have been documented within the tracheids of *Botryopteris antiqua* and *Rhexoxylon piatnitzkyi* (Krings *et al*., 2011; Sagasti & Bodnar, 2023). This led to the speculation of a complex plant-arthropod-fungus interaction, which has been well-documented in Permian woods (D'Rozario *et al*., 2011; Feng *et al*., 2017; Wei *et al*., 2019). However, upon re-examination, it was found that similar structures also occurred in a previously documented section of *Hansopteris uncinatus* (Fig. 3O), where coprolites were entirely absent (Zhou *et al*., 2021). Moreover, SEM-EDS analysis revealed impressions and compressions of crystals composed of Fe and S within the spheres (Fig. 3B, D, F, J), suggesting that these structures were not fungi but probably imprints of pyrite framboids. Pyrite mineralization has been documented previously in some Pennsylvanian plant cuticles, with the process assumed to be diagenetic (Zodrow & Mastalerz, 2009).

Acknowledgements

We appreciate the following in the Nanjing Institute of Geology and Palaeontology, Chinese Academy of Sciences (NIGPAS): Jing-Jing Tang for her help with photographing and stereomicroscopic observation; Le Yang for his assistance in making thin sections; and Yan Fang and Jing-Yi Yang for their support with SEM-EDS analysis. We thank the three anonymous reviewers for their constructive comments and valuable suggestions, which have significantly improved the quality of this paper. This study was funded by the National Natural Science Foundation of China (42172018) and the Youth Innovation Promotion Association of Chinese Academy of Sciences (2022312) to Wei-Ming Zhou, the Strategic Priority Research Program (B) of Chinese Academy of Sciences (XDB26000000) to Zhuo Feng and Jun Wang, and the Visiting Professorship for Senior International Scientists of Chinese Academy of Sciences (2016vea004) to Josef Pšenička.

References

Cai, C.Y., Tihelka, E., Giacomelli, M., Lawrence, J.F., Kundrata, R., Yamamoto, S., Thayer, M.K., Newton, A.F., Leschen, R.A.B., Gimmel, M.L., Lü, L., Engel, M.S., Bouchard, P., Huang, D.Y., Pisani, D. & Donoghue, P.C.J. (2022) Integrated phylogenomics and fossil data illuminate the evolution of beetles. *Royal Society Open Science*, 9 (3), 211771. https://doi.org/10.1098/rsos.211771

Cheng, Y.M., Yang, X.N. & Liu, F.X. (2021) A permineralized thamnopteroid rhizome (Osmundaceae) with coprolites from the Permian of Heilongjiang Province, northeast China: The most primitive record of Osmundaceae in Asia. *Review of Palaeobotany and Palynology*, 290, 104425. https://doi.org/10.1016/j.revpalbo.2021.104425

D'Rozario, A., Labandeira, C., Guo, W.Y., Yao, Y.F. & Li, C.S. (2011) Spatiotemporal extension of the Euramerican *Psaronius* component community to the Late Permian of Cathaysia: In situ coprolites in a *P. housuoensis* stem from Yunnan Province, southwest China. *Palaeogeography, Palaeoclimatology, Palaeoecology*, 306 (3-4), 127–133. https://doi.org/10.1016/j.palaeo.2011.04.009

Dunlop, J.A. & Garwood, R.J. (2017) Terrestrial invertebrates in the Rhynie chert ecosystem. *Philosophical Transactions of the Royal Society B-Biological Sciences*, 373 (1739), 20160493. https://doi.org/10.1098/rstb.2016.0493

Falcon-Lang, H.J., Labandeira, C. & Kirk, R. (2015) Herbivorous and detritivorous arthropod trace fossils associated with subhumid vegetation in the Middle Pennsylvanian of Southern Britain. *Palaios*, 30 (3), 192–206. https://doi.org/10.2110/palo.2014.082

Fang, Y.H., Qin, X., Liao, Q.G., Du, R., Luo, X.Z., Zhou, Q., Li, Z., Chen, H.C., Jin, W.T., Yuan, Y.N., Sun, P.B., Zhang, R., Zhang, J., Wang, L., Cheng, S.F., Yang, X.Y., Yan, Y.H., Zhang, X.T., Zhang, Z.H., Bai, S.N., Van de Peer, Y., Lucas, W.J., Huang, S.W. & Yan, J.B. (2021) The genome of homosporous maidenhair fern sheds light on the euphyllophyte evolution and defences. *Nature Plants*, 8 (9), 1024–1037. https://doi.org/10.1038/s41477-022-01222-x

Feng, Z., Bertling, M., Noll, R., Ślipiński, A. & Rößler, R. (2019) Beetle borings in wood with host response in early Permian conifers from Germany. *Paläontologische Zeitschrift*, 93 (3), 409–421. https://doi.org/10.1007/s12542-019-00476-9

Feng, Z., Wang, J., Rößler, R., Ślipiński, A. & Labandeira, C. (2017) Late Permian wood-borings reveal an intricate network of ecological relationships. *Nature Communications*, 8, 556. https://doi.org/10.1038/s41467-017-00696-0

Feng, Z., Wang, J., Zhou, W.M., Wan, M.L. & Pšenička, J. (2021) Plant-insect interactions in the early Permian Wuda Tuff Flora, North China. *Review of Palaeobotany and Palynology*, 294, 104269. https://doi.org/10.1016/j.revpalbo.2020.104269

Fletcher, T.L. & Salisbury, S.W. (2014) Probable oribatid mite (Acari: Oribatida) tunnels and faecal pellets in silicified conifer wood from the Upper Cretaceous (Cenomanian—Turonian) portion of the Winton Formation, central–western Queensland, Australia. *Alcheringa*, 38 (4), 541–545. https://doi.org/10.1080/03115518.2014.912557

Galtier, J. & Phillips, T.L. (2014) Evolutionary and ecological perspectives of Late Paleozoic ferns. Part III. Anachoropterid ferns (including *Anachoropteris*, *Tubicaulis*, the Sermayaceae, Kaplanopteridaceae and Psalixochlaenaceae). *Review of Palaeobotany and Palynology*, 205, 31–73.
https://doi.org/10.1016/j.revpalbo.2014.02.012

Goto, H.E. (1972) On the structure and function of the mouthparts of the soil-inhabiting collembolan *Folsomia candida*. *Biological Journal of the Linnean Society*, 4 (2), 147–168.
https://doi.org/10.1111/j.1095-8312.1972.tb00693.x

Hendrix, S.D. (1980) An evolutionary and ecological perspective of the insect fauna of ferns. *The American Naturalist*, 115 (2), 171–196.
https://doi.org/10.1086/283554

Holden, H.S. (1910) Note on a wounded *Myeloxylon*. *New Phytologist*, 9 (6-7), 253–257.
https://doi.org/10.1111/j.1469-8137.1910.tb05573.x

Holden, H.S. (1912) Some wound reactions in filicinean petioles. *Annals of Botany*, 26 (3), 777–794.
https://doi.org/10.1093/oxfordjournals.aob.a089416

Holden, H.S. (1931) Some observations on the wound reactions of *Ankyropteris corrugata*. *Botanical Journal of the Linnean Society*, 48 (325), 643–655.
https://doi.org/10.1111/j.1095-8339.1931.tb00597.x

Kim, K.W., Hyun, J.W. & Park, E.W. (2004) Cytology of cork layer formation of citrus and limited growth of *Elsinoe fawcettii* in scab lesions. *European Journal of Plant Pathology*, 110 (2), 129–138.
https://doi.org/10.1023/B:EJPP.0000015330.21280.4c

Krings, M., Dotzler, N., Galtier, J. & Taylor, T.N. (2011) Oldest fossil basidiomycete clamp connections. *Mycoscience*, 52 (1), 18–23.
https://doi.org/10.1007/s10267-010-0065-4

Laaß, M., Kretschmer, S., Leipner, A. & Hauschke, N. (2020) First evidence of arthropod herbivory in calamitalean stems from the Pennsylvanian of Germany. *Annales Societatis Geologorum Poloniae*, 90 (3), 219–246.
https://doi.org/10.14241/asgp.2020.14

Labandeira, C.C. (2006) The four phases of plant-arthropod associations in deep time. *Geologica Acta*, 4 (4), 409–438.

Labandeira, C.C. & Phillips, T.L. (1996) Insect fluid-feeding on Upper Pennsylvanian tree ferns (Palaeodictyoptera, Marattiales) and the early history of the piercing-and-sucking functional feeding group. *Annals of the Entomological Society of America*, 89 (2), 157–183.
https://doi.org/10.1093/aesa/89.2.157

Labandeira, C.C., Phillips, T.L. & Norton, R.A. (1997) Oribatid mites and the decomposition of plant tissues in Paleozoic coal-swamp forests. *Palaios*, 12 (4), 319–353.
https://doi.org/10.2307/3515334

Lesnikowska, A.D. (1990) Evidence of herbivory in tree-fern petioles from the Calhoun Coal (Upper Pennsylvanian) of Illinois. *Palaios*, 5 (1), 76–80.
https://doi.org/10.2307/3514997

Nejat, N. & Mantri, N. (2017) Plant immune system: Crosstalk between responses to biotic and abiotic stresses the missing link in understanding plant defence. *Current Issues in Molecular Biology*, 23, 1–16.
https://doi.org/10.21775/cimb.023.001

Ozeretskovskaya, O.L., Vasyukova, N.I., Chalenko, G.I., Gerasimova, N.G., Revina, T.A. & Valueva, T.A. (2009) Wound healing and induced resistance in potato tubers. *Applied Biochemistry and Microbiology*, 45 (2), 199–203.
https://doi.org/10.1134/S0003683809020148

Pšenička, J., Wang, J., Bek, J., Pfefferkorn, H.W., Opluštil, S., Zhou, W.M., Frojdová, J.V. & Libertín, M. (2021) A zygopterid fern with fertile and vegetative parts in anatomical and compression preservation from the earliest Permian of Inner Mongolia, China. *Review of Palaeobotany and Palynology*, 294, 104382.
https://doi.org/10.1016/j.revpalbo.2021.104382

Putz, F.E. (1980) Lianas vs. trees. *Biotropica*, 12 (3), 224–225.
https://doi.org/10.2307/2387978

Rex, G.M. (1986) The preservation and paleoecology of the Lower Carboniferous silicified plant deposits at Esnost, near Autun, France. *Geobios*, 19 (6), 773–800.
https://doi.org/10.1016/s0016-6995(86)80107-3

Rößler, R. (2000) The late Palaeozoic tree fern *Psaronius*: An ecosystem unto itself. *Review of Palaeobotany and Palynology*, 108 (1-2), 55–74.
https://doi.org/10.1016/s0034-6667(99)00033-0

Rößler, R., Feng, Z. & Noll, R. (2012) The largest calamite and its growth architecture—*Arthropitys bistriata* from the Early Permian Petrified Forest of Chemnitz. *Review of Palaeobotany and Palynology*, 185, 64–78.
https://doi.org/10.1016/j.revpalbo.2012.07.018

Sagasti, A.J. & Bodnar, J. (2023) Biological decay by microorganisms in stems from the Upper Triassic Ischigualasto Formation (San Juan Province, Argentina): A striking microbial diversity in Carnian-Norian terrestrial ecosystems. *Review of Palaeobotany and Palynology*, 315, 104915.
https://doi.org/10.1016/j.revpalbo.2023.104915

Schmitz, M.D., Pfefferkorn, H.W., Shen, S.Z. & Wang, J. (2021) A volcanic tuff near the Carboniferous-Permian boundary, Taiyuan Formation, North China: Radioisotopic dating and global correlation. *Review of Palaeobotany and Palynology*, 294, 1–6.
https://doi.org/10.1016/j.revpalbo.2020.104244

Scott, A.C., Stephenson, J. & Chaloner, W.G. (1992) Interaction and coevolution of plants and arthropods during the Paleozoic and Mesozoic. *Philosophical Transactions of the Royal Society B-Biological Sciences*, 335 (1274), 129–165.
https://doi.org/10.1098/rstb.1992.0016

Scott, A.C. & Taylor, T.N. (1983) Plant animal interactions during the Upper Carboniferous. *The Botanical Review*, 49 (3), 259–307.
https://doi.org/10.1007/bf02861089

Slater, B.J., McLoughlin, S. & Hilton, J. (2012) Animal-plant interactions in a Middle Permian permineralised peat of the Bainmedart Coal Measures, Prince Charles Mountains, Antarctica. *Palaeogeography, Palaeoclimatology, Palaeoecology*, 363, 109–126. https://doi.org/10.1016/j.palaeo.2012.08.018

Stopes, M.C. (1907) A note on wounded calamites. *Annals of Botany*, 21 (81-84), 277–281. https://doi.org/10.1093/oxfordjournals.aob.a089133

Wang, J., Pfefferkorn, H.W., Oplustil, S. & Kerp, H. (2021) Permian "vegetational Pompeii": A peat-forming in situ preserved forest from the Wuda Coalfield, Inner Mongolia, China—Introduction to a volume of detailed studies. *Review of Palaeobotany and Palynology*, 294, 104502. https://doi.org/10.1016/j.revpalbo.2021.104502

Weaver, L., McLoughlin, S. & Drinnan, A.N. (1997) Fossil woods from the Upper Permian Bainmedart Coal Measures, northern Prince Charles Mountains, East Antarctica. *AGSO Journal of Australian Geology and Geophysics*, 16 (5), 655–676.

Wei, H.B., Gou, X.D., Yang, J.Y. & Feng, Z. (2019) Fungi-plant-arthropods interactions in a new conifer wood from the uppermost Permian of China reveal complex ecological relationships and trophic networks. *Review of Palaeobotany and Palynology*, 271, 104100. https://doi.org/10.1016/j.revpalbo.2019.07.005

Zhou, W.M., He, X.Y., Wang, S.J., Pšenička, J., Rößler, R., Rothwell, G.W., Galtier, J., Hilton, J. & Wang, J. (2023a) (3005) Proposal to conserve the name *Botryopteris* Renault (fossil *Pteridophyta*) against *Botryopteris* C. Presl (*Ophioglossaceae*). *Taxon*, 72 (6), 1377–1379. https://doi.org/10.1002/tax.13097

Zhou, W.M., Li, D.D., Pšenička, J., Boyce, C.K. & Wang, J. (2019) A left-handed fern twiner in a Permian swamp forest. *Current Biology*, 29 (22), R1172–R1173. https://doi.org/10.1016/j.cub.2019.10.005

Zhou, W.M., Li, D.D., Pšenička, J., Boyce, C.K., Wang, S.J. & Wang, J. (2022a) *Diodonopteris virgulata* sp. nov., a climbing fern from the early Permian Wuda Tuff Flora and its paleoecology. *Review of Palaeobotany and Palynology*, 304, 104699. https://doi.org/10.1016/j.revpalbo.2022.104699

Zhou, W.M., Pšenička, J., Bek, J., Libertin, M., Wang, S.J. & Wang, J. (2023b) A new species of *Botryopteridium* Doweld from the early Permian Wuda Tuff Flora and its evolutionary significance. *Review of Palaeobotany and Palynology*, 311, 104849. https://doi.org/10.1016/j.revpalbo.2023.104849

Zhou, W.M., Pšenička, J., Bek, J., Wan, M.L., Boyce, C.K. & Wang, J. (2021) A new anachoropterid fern from the Asselian (Cisuralian) Wuda Tuff Flora. *Review of Palaeobotany and Palynology*, 294, 104346. https://doi.org/10.1016/j.revpalbo.2020.104346

Zhou, W.M., Pšenička, J., Frojdová, J.V., Wang, J., Wan, M.L. & Feng, Z. (2024) Two anachoropterid fern rachises from the in situ volcanic ash of the Whetstone Horizon (Kladno Formation, Pennsylvanian), Radnice Basin, Czech Republic. *Palaeoworld*, 33 (2), 341–362. https://doi.org/10.1016/j.palwor.2023.02.003

Zhou, W.M., Wan, M.L., Pšenička, J. & Wang, J. (2022b) Discovery of coprolites in an Early Permian fern mesophyll. *Palaeoentomology*, 5 (1), 1–5. https://doi.org/10.11646/palaeoentomology.5.1.1

Zodrow, E.L. & Mastalerz, M. (2009) A proposed origin for fossilized Pennsylvanian plant cuticles by pyrite oxidation (Sydney Coalfield, Nova Scotia, Canada). *Bulletin of Geosciences*, 84 (2), 227–240. https://doi.org/10.3140/bull.geosci.1094